Effect of molecular weight on the crystallization behaviour of poly(aryl ether ether ketone): a differential scanning calorimetry study*

M. Day, Y. Deslandes, J. Roovers† and T. Suprunchuk
Division of Chemistry, National Research Council of Canada, Ottawa, Ontario, Canada K1A 0R6
(Received 2 April 1990; accepted 13 June 1990)

The effect of molecular weight on the kinetics of the crystallization of poly(aryl ether ether ketone) has been investigated by means of a series of fractions of relatively narrow molecular-weight distribution. In this study the crystallization has been monitored by differential scanning calorimetry (d.s.c.). Analysis of the sigmoidal crystallization curves by means of the Avrami equation leads to $n \approx 2$. In order to obtain a uniform set of rate constants (k), small adjustments in the zero time were made. Measurements have been made of the crystallization of amorphous samples just above the glass transition temperature. The temperature dependence of the observed rate constants follows a Vogel equation, $\log k = U^*/2.3R(T_c - T_\infty)$, where $U^* \approx 4500$ cal mol^{-1} and $T_\infty = T_g - 55$. These parameters are consistent with the universal WLF parameters. The experimental glass transition temperature of each sample has been used. It is found that the rate of crystallization considered under iso-free-volume conditions depends on M^{-2} as expected for a diffusion-controlled process that involves entangled linear polymers. This conclusion is supported by an analysis of the onset temperature of crystallization in dynamic d.s.c. scans of the different molecular-weight samples. In another series of experiments the crystallization rates have been measured below the melting point of the samples. Analysis of the temperature dependence of the rate constants reveals that high-molecular-weight polymers crystallize at lower temperature ($T_c = 270$–290°C) according to regime III. Low-molecular-weight samples require higher temperatures in order to measure the rates of crystallization ($T_c > 300$°C). The temperature dependence of the rate constants suggests that in that case crystallization occurs according to regime II. One sample ($M_w = 32\,000$) showed a regime III–regime II transition at about 298°C. These conclusions are not drastically affected by reasonable variations in U^*, T_∞ and the equilibrium melting temperature T_m°.

(Keywords: poly(ether ether ketone); differential scanning calorimetry; crystallization kinetics)

INTRODUCTION

Poly(aryl ether ether ketone) (PEEK) is a semicrystalline polymer with a high melting temperature. Combined with good thermal stability, the semicrystalline nature makes PEEK a high-performance thermoplastic for use in advanced composites. The mechanical properties of PEEK depend crucially on the crystallinity and morphology of the polymer. It is therefore essential to understand the crystallization behaviour in order to obtain materials with controlled and reproducible properties.

The crystallization behaviour of PEEK has been studied by several authors. Differential scanning calorimetry (d.s.c.) has been the major tool[1–21]. Light microscopy has also been used[1,22,23]. These techniques are supplemented by electron microscopy[1,22,24–27] and X-ray work[5,22,27–36]. Two interesting problems have arisen out of this work. The first one is the observed dependence of the unit-cell dimensions on the temperature of crystallization and/or annealing[30,33]. We feel that this may be related to the crystallization mechanism and may be reflected in the kinetics of crystallization. The second problem is related to the complex melting that is often observed in PEEK. The complex melting endotherm has been explained as arising solely from the presence of crystallites with different degrees of perfection[4,17]. Others have claimed that originally there is one type of poorly developed crystallite that is continuously reorganized during a d.s.c. scan[2,8,10]. It is quite likely that in many instances both phenomena occur, i.e. crystallites with different degrees of perfection melt and recrystallize to different degrees during the d.s.c. scan[14]. A better understanding of the kinetics of crystallization as a function of molecular weight (MW) and temperature would greatly help in the elucidation of the complex phenomena that happen during a d.s.c. scan.

The kinetics of the crystallization of PEEK has been less well studied and most of the studies have been on commercial samples with poorly defined molecular characteristics[1,3,4,6,7,12,13,19,20]. In the present study we have examined the influence of the molecular weight of PEEK on its bulk crystallization kinetics. A comparison with the kinetics of crystallization of commercial PEEK is included. The molecular-weight dependence of the glass transition temperature, which is required for analysis of the crystallization data, has also been determined. We have, however, failed to resolve the dependence of the

* Issued as NRCC report no. 32527
† To whom correspondence should be addressed

0032-3861/91/071258-09

equilibrium melting temperature T_m° on molecular weight. The possible effect of neglecting this parameter will be discussed.

EXPERIMENTAL

The PEEK samples employed in this study were prepared in our laboratory by way of the ketimine prepolymer[37,38]. Details of the synthesis, fractionation and characterization are reported elsewhere[38]. The samples used range in *MW* between 4600 and 79 500. Their polydispersity index M_w/M_n ranges from 1.2 to 1.5.

The thermal properties of the PEEK samples were measured with a DuPont model 910 d.s.c. coupled to a DuPont 2100 data analysis system. The d.s.c. was calibrated with indium and zinc initially and at several occasions during the study. In all cases the polymer sample weights were maintained in the 5–7 mg range and recorded to ± 0.01 mg in aluminium pans. All experiments were conducted in a flowing nitrogen atmosphere of 50 ml min^{-1}.

Glass transition temperatures were measured on samples heated from 30 to 400°C at 10°C min^{-1}. The samples were then rapidly removed from the d.s.c. cell and quenched in liquid nitrogen to make a totally amorphous sample. T_g was then determined on the amorphous samples in a d.s.c. run from 30 to 400°C at a heating rate of 10°C min^{-1}. T_g was taken as the midpoint of the transition. Scans at other rates were used to eliminate instrumental factors by linear extrapolation to zero heating rate.

For isothermal crystallization from the glass, amorphous samples were prepared as described for the T_g measurements. The d.s.c. cell was then set at the desired isothermal crystallization temperature. The amorphous sample was then rapidly inserted and the crystallization exotherm recorded. The temperature range was chosen so that total crystallization took from 4 to 90 min. For isothermal crystallization from the melt, the sample was initially heated from 30 to 400°C at 10°C min^{-1}. No further attempts were made to destroy persisting nuclei as this is known to affect the crystallization kinetics as a result of molecular changes[19,23]. The sample was then rapidly cooled with ice to the selected crystallization temperature. A temperature program was developed by means of a silica sample, which resulted in a temporary undercooling of about 0.3°C. The total time of crystallization was between 5 and 120 min.

RESULTS

Glass transition temperature

Figure 1 shows typical d.s.c. scans of amorphous PEEK samples of various molecular weights. The changes in the heat capacity associated with T_g are seen around 150°C. Experimental data on T_g are collected in *Table 1*.

It is well known that the glass transition temperature of a polymer increases with increasing number-average molecular weight to a high-molecular-weight limiting value (T_g^∞). Many relations have been proposed for this dependence. Ueberreiter and Kanig proposed that:

$$(1/T_g) = (1/T_g^\infty) + KM_n^{-1} \quad (1)$$

This is shown in *Figure 2*. From the intercept $T_g^\infty = 152.2$°C at 10°C min^{-1} heating rate. Correction to zero heating rate lowers this to $T_g^\infty = 148.0$°C. Note the strong dependence of T_g on molecular weight. The value of T_g quoted for commercial PEEK is lower than T_g^∞.

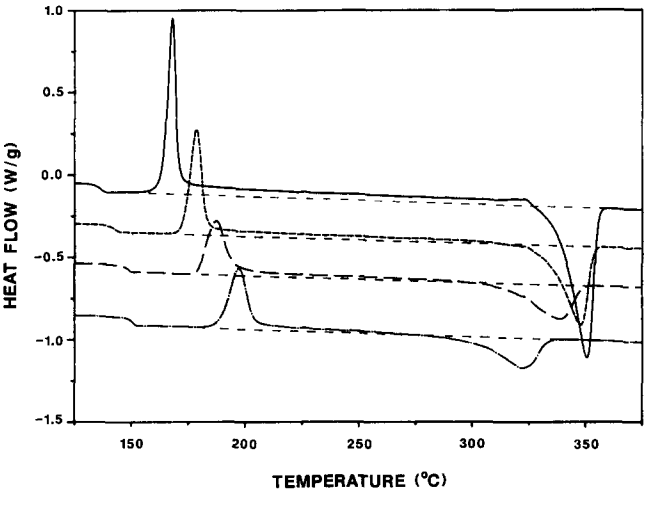

Figure 1 D.s.c. scans of amorphous samples of PEEK fractions. From top to bottom: 2D/1, 2C/1, 1B/1 and 4D/1. Individual curves are displaced vertically for clarity

Table 1 Characteristics of PEEK fractions

Sample	M_w	M_n[a]	T_g (°C)[b]	T_c' (°C)[c]	ΔH_c (J g^{-1})[d]
1A22/1	55 500	34 900	150.5	189.5	22
1B/1	32 000	21 500	148.6	182.1	22
1C/1	13 500	9 000	143.6	173.0	30
2C/1	18 000	14 500	143	172.7	25
2D/1	8 300	7 000	136	163.9	31
4D/1	79 500	60 200	151	189.0	22
4E/1	39 200	30 900	148	183.6	23
5C/1	7 800	5 700	135.2	161.8	26
5D/1	4 400	3 500	124.5	150.1	(20)

[a]Based on M_w from light scattering and M_w/M_n from g.p.c.[38]
[b]T_g measured at 10°C min^{-1}
[c]Temperature of onset of crystallization in d.s.c. at 10°C min^{-1}
[d]Heat of crystallization on scanning amorphous polymer at 10°C min^{-1}

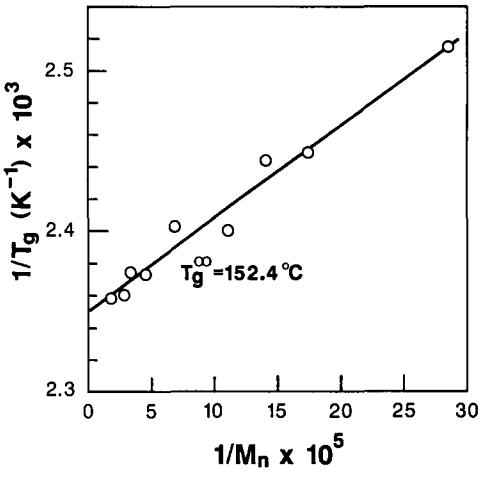

Figure 2 Ueberreiter–Kanig plot of glass transition temperature (K) against number-average molecular weight for fractions of PEEK

This is of course due to the wide molecular-weight distribution and the rather low value of M_n in the commercial polymer ($M_n \approx 14\,000$)[10].

Overall aspects of crystallization kinetics

Essentially two ranges of temperature are amenable to measurement of crystallization kinetics. The first is the range 145–190°C, where amorphous samples crystallize just above the glass transition temperature. This is called crystallization from the glass. The crystallization rate increases with temperature. The second temperature range is between 235 and 320°C, where the sample is cooled from the melt. We call this crystallization from the melt. In this temperature range the crystallization rate decreases with an increase in temperature. The crystallization half-times are shown for all the samples as a function of temperature in *Figure 3*. This representation is independent of any particular theory for the crystallization mechanism. In *Figure 3* the maximum rate of crystallization is at about 220–230°C but is not experimentally accessible[1]. It is foreseeable that the complete temperature range of crystallization would be accessible for higher-molecular-weight or crosslinked PEEK. The maximum rate of crystallization was recently observed for poly(*p*-phenylene sulphide) (PPS)[39]. From *Figure 3* it can be seen that at all temperatures the low-*MW* fractions crystallize faster than high-*MW* fractions. This suggests that the crystallization rates are governed by kinetic rather than thermodynamic effects.

In general, the rate constant of crystallization is written as:

$$k = k_0 \exp\left(\frac{-U^*}{R(T_c - T_\infty)}\right) \exp\left(\frac{-K_g}{T_c(\Delta T)f}\right) \qquad (2)$$

where T_c is the crystallization temperature; $T_\infty = T_g - C$, where C is a constant to be discussed below; $\Delta T = (T_m^\circ - T_c)$ and represents the degree of undercooling below T_m°, the thermodynamic melting temperature of an infinitely thick lamella; and the factor f is a correction term introduced to account for the temperature dependence of the heat of crystallization. In crystallization from the glass the first exponential term dominates, i.e. the local mobility governs the rate of crystallization. In crystallization from the melt the second exponential term is the more important since the crystallization rate is governed by the rate of nucleation, which depends on the degree of undercooling. Equation (2) will produce curves of the form seen in *Figure 3*.

Crystallization from the glass

Quenched samples of PEEK fractions were crystallized in the d.s.c. slightly above the glass transition temperature of the polymer. The d.s.c. exotherms were analysed according to the method of Avrami. Most weight was put on data below 50% relative crystallinity, as deviations from Avrami kinetics are often observed in the final stages of crystallization. An example of the crystallization is shown in *Figure 4* together with its Avrami analysis. In order to obtain a consistent Avrami exponent, $n = 2$, the zero time of crystallization was sometimes adjusted, usually by a fraction of the time at which the first data point was recorded. The rate constants of crystallization k (s^{-2}) are given in *Table 2*. Sample 2D/1 gave consistently $n = 2.4 \pm 0.2$ rather than 2.0. We are not sure that this sample is completely amorphous after the quenching process. Other lower-molecular-weight fractions definitely revealed some crystallinity after quenching from the melt at 400°C. Although the rates of

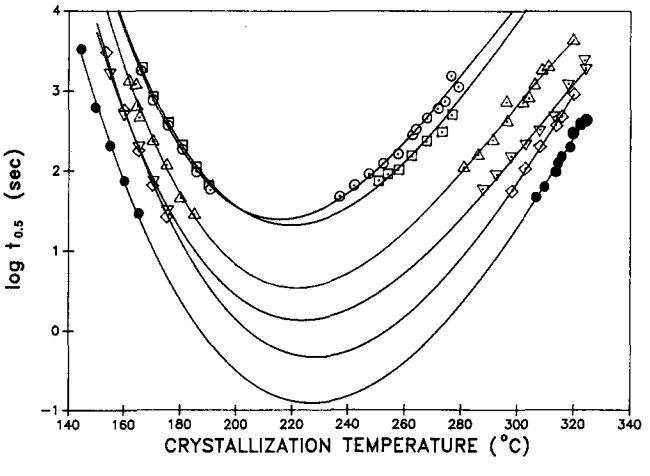

Figure 3 Log(crystallization half-time) *versus* temperature for the crystallization of PEEK fractions: (●) 2D/1; (◇) 1C/1; (▽) 2C/1; (△) 1B/1; (□) 1A22/1; (○) 4D/1. Lines are drawn as a guide to the eye only

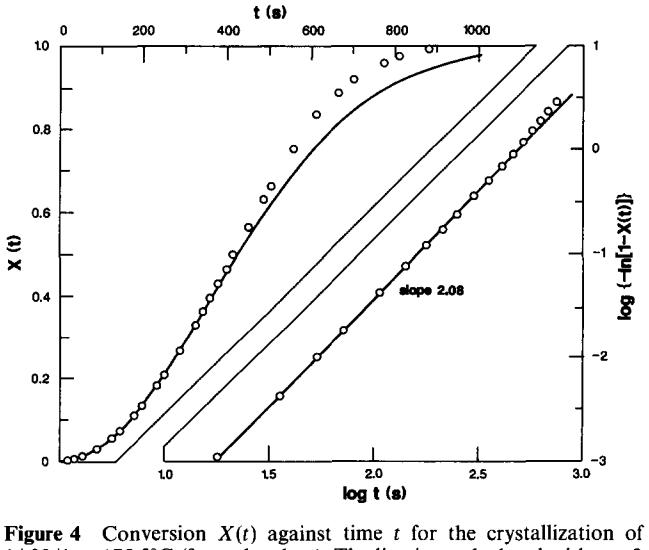

Figure 4 Conversion $X(t)$ against time t for the crystallization of 1A22/1 at 175.5°C (from the glass). The line is recalculated with $n = 2$ and log k = −5.425. Circles are experimental points. On the left is the corresponding Avrami analysis. Slope $n = 2.08$

Table 2 Crystallization from the glass

Sample	Temperature (°C)	ΔH (J g^{-1})	log[k (s^{-2})]
2D/1	144.5	15.1 (14.3)	−7.40
T_g = 136.0°C	149.7	19.2	−6.00
	154.8	25.5	−5.00
	159.9	23.3	−4.00
	165.1	25.4	−3.16
	170.3	22.0	−2.40
1C/1	155.2	11.8	−6.62(?)
T_g = 143.6°C	160.3	9.0	−5.70
	165.3	22.2	−4.695
	170.3	23.1	−3.84
	175.4	22.2	−3.045
2C/1	155.1	19.2	−6.62
T_g = 143°C	160.2	18.3	−5.75
	165.2	22.4	−4.885
	170.4	23.6	−3.965
	175.4	22.3	−3.185
1B/1	164.1	8.7	−6.30
T_g = 148.6°C	165.3	13.5	−5.50
	170.6	10.9	−4.86
	175.1	13.0	−4.30
	180.2	15.2	−3.48
	185.0	13.5	−3.18
1A22/1	166.4	11.5	−5.86
T_g = 150.5°C	170.4	11.2	−5.70
	175.5	12.8	−5.425
	180.5	14.3	−4.80
	185.6	15.0	−4.275
	190.7	15.7	−3.84
4D/1	165.7	10.6	−6.735
T_g = 151°C	170.3	8.6	−5.995
	175.3	12.1	−5.39
	180.6	15.3	−4.76
	185.5	14.8	−4.18
	190.6	14.4	−3.70

crystallization of this sample are not inconsistent with those of the other samples, as will be shown later, we do not put great weight on these results. Dependence of n on molecular weight has also been observed for polyethylene[40].

The overall degree of crystallization obtained in the isothermal crystallization from the glass is low. The experimental enthalpies of crystallization are given in *Table 2*. It can be seen that the enthalpies of crystallization increase with the temperature of crystallization. Within experimental error the enthalpy of crystallization is constant when $k \geqslant 10^{-5}\,s^{-2}$. Low enthalpies are usually observed for crystallization only slightly above T_g. In fact T_g may increase during crystallization and reduce the necessary chain mobility. From *Table 2* it can also be seen that the enthalpy of crystallization decreases with increasing molecular weight. Based on a heat of crystallization of 130 J g^{-1} at 395°C[1], and crudely assuming the heat of crystallization to be independent of temperature, the overall degree of crystallinity varies from 17% to about 12% for the highest molecular weight. It can therefore be stressed that the total crystallinity plotted in *Figure 4* represents only 10% absolute crystallinity in the sample.

According to equation (2) the rates of crystallization from the glass should depend on temperature as:

$$k = k_0' \exp\left(\frac{-U^*}{R(T_c - T_\infty)}\right) \qquad (3)$$

Here we assume that at very low temperatures the second exponential term provides only a minor shift, which is incorporated into k_0'.

Plots of log k against $T_c - T_\infty$ are shown in *Figure 5*. T_∞ has been calculated with the T_g of each sample from the Ueberreiter–Kanig relation (equation (1)). The constant in $T_\infty = T_g - C$ is taken to be 55°C. Because the crystallization rate is plotted against temperature relative to each sample's individual glass transition temperature, it is expected that all slopes in *Figure 5* are identical. Experimentally slopes vary between 1010 and 908 K with a tendency to decrease with increasing molecular weight. Values of $U^* = 4600$ to 4140 cal mol^{-1} are found. We feel that the experimental error in k is too large to refine the analysis, e.g. by assuming other values of C.

The temperature dependence of equation (3) is of the Vogel type which, in the Williams–Landel–Ferry (WLF) form, is used to describe the temperature dependence of the viscoelastic properties of polymer melts[41]. With $C_2^\circ = 55$ one obtains, from *Figure 5*, C_1° = slope/C_2° = 15.37 to 18.3. Recall that the original WLF treatment proposed C_1° and C_2° to be universal constants equal to 17.7 and 51.6, respectively. This comparison of the temperature dependence of the crystallization rate with that of the melt viscosity strongly suggests that crystallization rates are dominated by chain mobility. Other studies of rate of crystallization have suggested other coefficients for temperature dependence[42,43]. It is not certain that C_1° and C_2° are universal constants; it would be best to determine them independently by viscoelastic measurement, but this seems to be elusive at the moment for crystallizing polymers.

As in relaxation-time experiments, the foregoing

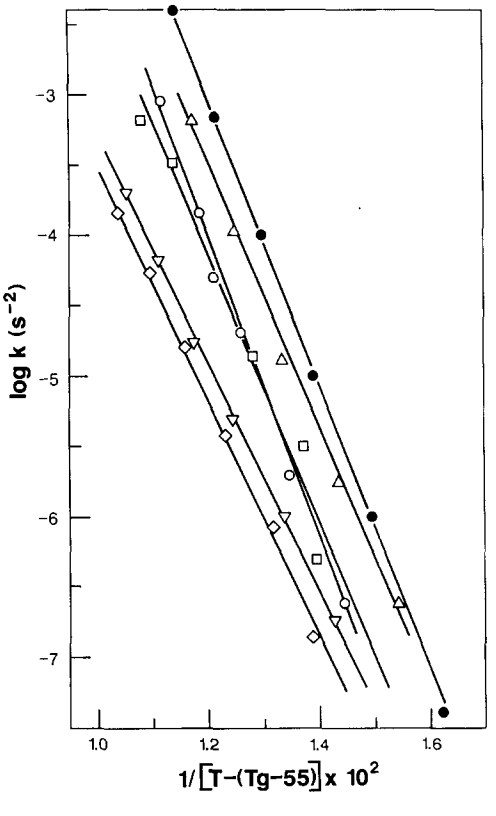

Figure 5 Temperature dependence of the crystallization rate constants obtained from crystallizations from the glass: (●) 2D/1; (△) 2C/1; (○) 1C/1; (□) 1B/1; (▽) 4D/1; (◇) 1A22/1

discussion suggests that the molecular-weight dependence of the crystallization rate has to be studied at $T_c - T_g$ = constant rather than at constant temperature. This is shown in *Figure 6* for $1/(T_c - T_\infty) = 1.30 \times 10^{-2}$. Although the precision of the results leaves something to be desired, it is found that the rate of crystallization depends on M_w^{-2}. This is in agreement with a rate of crystallization that depends on the diffusion rate of entangled linear chains[44]. Viscoelastic measurements indicate that PEEKs in the molecular-weight range studied here are indeed entangled, with the possible exception of the lowest *MW* sample[45]. This can also be deduced from the generally low M_e values observed for amorphous polymers that have phenylene groups in the main chain[45].

Crystallization from the glass during the d.s.c. scan

It can be seen from *Figure 1* that the extent of crystallization decrease with increasing molecular weight, as already observed in the isothermal crystallization. The heats of crystallization (scanned at 10°C min^{-1}) are given in *Table 1*. In general, they are somewhat higher than those observed in the isothermal crystallization from the glass, but this is of no great significance because the temperature range of the isothermal crystallization is limited.

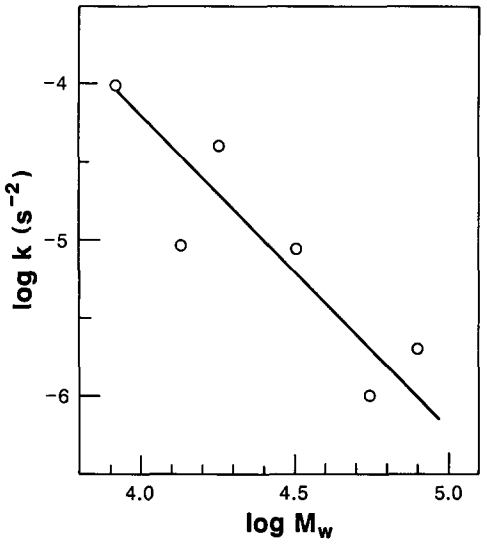

Figure 6 Log–log plot of the crystallization rate constant at constant iso-free-volume against molecular weight. The line drawn has slope of −2

It is of interest to investigate the assumption that the onset of a measurable crystallization during a d.s.c. scan occurs at the temperature at which all samples have the same diffusion coefficient. The diffusion coefficient D_0 depends inversely on the monomeric friction coefficient, which is strongly dependent on temperature, and on the molecular weight. Accordingly:

$$D_0 = [p(f_0)]^{-1} q(M) \quad (4)$$

The temperature dependence of the friction coefficient is given by equation (3) and the data shown in *Figure 5*. The molecular-weight dependence according to *Figure 6* is given by $q(M) \propto M^{-2}$. In *Table 3*, f_0 is calculated with the standard WLF equation at T_c', the onset of crystallization temperature of each sample. One sample, 5C/1, is then taken as a reference sample and f_0/f_{0R}, $(M/M_R)^2$ and their product are calculated. If diffusion is indeed the rate-controlling process, then $R = (f_0/f_{0R}) \times (M/M_R)^2$ is expected to be unity.

Although there is appreciable scatter, a small dependence of R on molecular weight is observed. It suggests that crystallization of high-molecular-weight samples starts at a slightly lower temperature. Note, however, that their crystallization occurs over a somewhat wider temperature range.

Crystallization from the melt

Typical Avrami analyses of the melt crystallization are shown for 1A22/1 in *Figure 7*. The Avrami exponent was normalized to $n = 2$, by small changes (−6 to 50 s) in the initial zero time of crystallization. The Avrami kinetics are followed to about 60–70% crystallization. Beyond 70% crystallization the rate of crystallization appears to slow down. It is worth while to recalculate the crystallization from the Avrami parameter. This is shown in *Figure 8*. By adjusting the Avrami exponent, the fit has suffered slightly but the deviation at 60–70% conversion is still clearly visible. As for crystallization from the glass, the absolute degree of crystallization is much less than 100%. Based on $\Delta H_f = 130$ J g^{-1} for the melting of pure crystalline PEEK[1], crystallinities between 15 and 50% are observed as given in *Table 4*. The degree of crystallization clearly decreases with increasing molecular weight. The crystallinity varies little with crystalliza-

Table 3 Analysis of dynamic crystallization results

Sample	T_c' (°C)[a]	log f_0[b]	f_0/f_{0R}	$(M/M_R)^2$	R[c]
1A22/1	189.5	−7.507	0.0285	50.63	1.44
1B/1	182.1	−6.665	0.125	16.83	2.10
1C/1	173.0	−6.330	0.428	3.00	1.28
2C/1	172.7	−5.371	0.390	5.33	2.08
2D/1	163.9	−6.120	0.694	1.13	0.78
4D/1	189.0	−7.396	0.0368	103.9	3.82
4E/1	183.6	−7.120	0.0695	25.3	1.76
5C/1[d]	161.8	−5.962	1.000	1.0	1.0
5D/1	150.1	−5.813	1.408	0.32	0.45

[a]Apparent temperature of onset of crystallization
[b]Calculated with equation (3), the original WLF constants, $T_c = T_c'$ and the individual T_g of each sample
[c]$R = (f_0/f_{0R})(M/M_R)^2$
[d]Taken as the reference sample

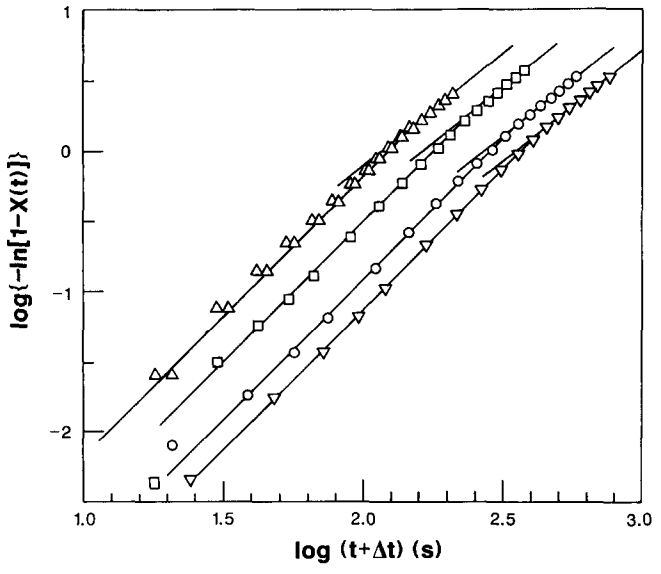

Figure 7 Avrami plot for crystallization in the melt of sample 1A22/1. The individual corrections to obtain $n = 2$ are: (Δ) 257.7°C, $\Delta t = 9$ s; (□) 262.4°C, $\Delta t = 6$ s; (○) 267.7°C, $\Delta t = -15$ s; (▽) 273.1°C, $\Delta t = 0$ s

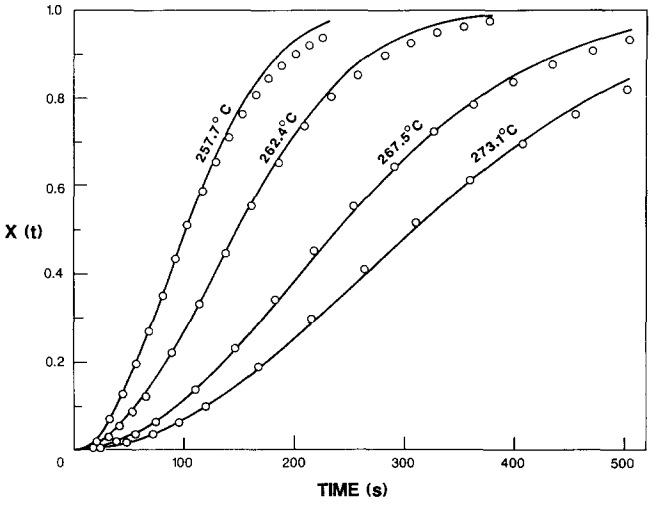

Figure 8 Conversion *versus* time for crystallization from the melt of sample 1A22/1. Circles are experimental data. Lines are recalculated with $n = 2$

tion temperature. A small decrease at low T_c is noticeable, however. This is consistent with the observation that annealing samples at higher temperature usually increases the degree of crystallinity. Note, however, that the undercooling used varies considerably for the samples. It is larger for the high-*MW* samples. At constant temperature the low-*MW* samples crystallize faster, as shown in *Figure 3*.

The rates of crystallization from the melt at different temperatures have been analysed according to equation (2). Equation (2) is first rewritten in a slightly different form according to:

$$\log k + \frac{U^*}{2.3R(T_c - T_\infty)} = \log k_0 - \frac{K_g}{2.303T_c(\Delta T)f} \quad (5)$$

Values of U^* and T_∞ are those derived from the study of the crystallization from the glass as described in the previous section. A correction factor f equal to $2T_c/(T_m^\circ + T_c)$ is applied. It should be stressed that $T_m^\circ = 395$°C has been used for all fractions[1].

A test of the crystallization rate constants according to equation (5) is shown in *Figure 9*. The data are interpreted as showing two types of behaviour. The high-molecular-weight samples have a slope $-K_g/2.303 = -(1.3 \pm 0.1) \times 10^6$ (K^2). The low-molecular-weight samples have a slope $-K_g/2.303 = -(6 \pm 0.5) \times 10^5$ (K^2). The data of sample 1B/1′ are interpreted as consisting of two lines. At low temperature, $-K_g/2.303 = -1.0 \times 10^6$ K^2, similar to the slope found for high-*MW* samples. At high temperatures the slope is about one-half, $-K_g/2.303 = -5.6 \times 10^5$ K^2, as also found for the low-*MW* samples. The transition is at approximately 298°C. Values of K_g for each sample are given in the second column of *Table 5*.

Table 4 Crystallization from the melt

Sample	T_c (°C)	ΔH (J g^{-1})	log[k (s^{-2})]
2D/1	306.7	63.8	−3.493
	309.7	57.6	−3.796
	313.6	60.7	−4.178
	314.5	58.9	−4.385
	315.8	65.4	−4.484
	317.8	65.6	−4.756
	319.0	68.0	−4.725
	319.5	65.9	−5.167
	322.8	62.9	−5.561
	324.0	78.1	−5.348
1C/1	298.2	41.7	−3.605
	302.9	52.7	−4.197
	308.4	56.1	−4.795
	313.5	51.3	−5.330
2C/1	287.6	43.2	−3.697
	292.7	45.8	−4.053
	297.8	50.2	−4.560
	302.8	49.3	−4.882
	308.0	53.8	−5.212
	312.9	47.7	−5.531
	315.8	60.9	−6.028
	318.2	58.1	−6.270
	323.9	53.2	−6.903
1B/1′	280.9	40.9	−4.219
	285.9	38.8	−4.545
	286.0	40.1	−5.049
	291.2	38.8	−4.991
	296.1	40.0	−5.766
	296.1	37.0	−5.958
	296.1	37.6	−5.808
	296.1	36.6	−5.415
	302.2	36.3	−5.925
	304.1	39.2	−5.967
	304.2	36.0	−6.773
	306.2	21.1	−6.402
	309.0	42.2	−6.695
	311.2	32.8	−6.739
1A22/1	250.8	22.8	−3.924
	254.0	25.6	−4.053
	257.7	24.1	−4.167
	262.4	25.9	−4.505
	267.5	25.6	−4.908
	273.1	24.2	−5.129
	276.5	32.9	−5.500
	279.0	23.4	−6.333
4D/1	236.9	17.9	−3.550
	242.0	19.1	−3.745
	247.2	26.5	−4.021
	252.3	21.8	−4.318
	257.5	20.6	−4.635
	262.7	22.2	−5.041
	267.8	21.7	−5.515
	271.7	23.7	−5.687
	274.2	24.2	−5.860
	276.5	29.4	−6.323

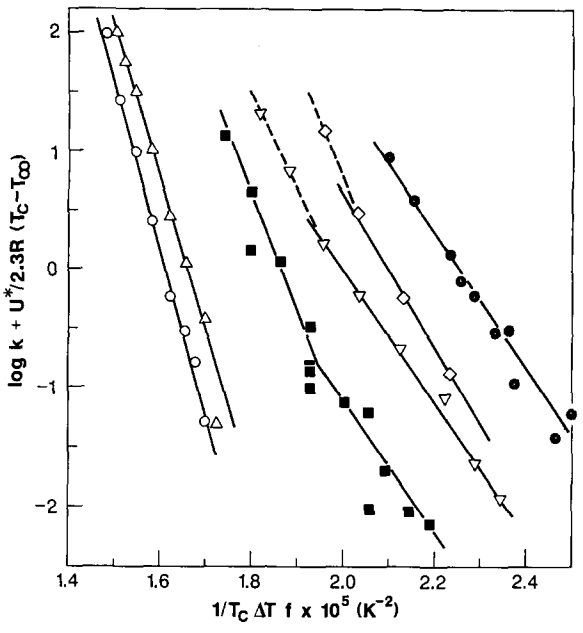

Figure 9 Kinetic analysis of melt crystallization rate constants, for $U^* = 4500$ cal mol^{-1}, $T_\infty = T_g - 55$°C and $T_m^\circ = 395$°C: (○) 4D/1; (△) 1A22/1; (■) 1B/1'; (▽) 2C/1; (◇) 1C/1; (●) 2D/1

DISCUSSION

In this study we have made an effort to extract values of crystallization rate constants from experimental d.s.c. crystallization curves correctly. This included paying attention to the initial disturbance in the d.s.c. trace when the temperature is changed to the isothermal crystallization temperature either from the glass or from the melt.

In reaching the crystallization temperature from below (crystallization from the glass), fewer problems were encountered because the crystallization rate increases with increasing temperature. However, in the crystallization from the melt, the isothermal crystallization temperature has to be reached with a limited undercooling during the shortest possible time in order to obtain a stable signal output before changes in heat flow due to crystallization are recorded. This severely limits the time over which crystallization kinetics can be followed and therefore limits the temperature range over which data can be collected. If such precautions are not taken, variable values of n in the Avrami plots are obtained as a function of temperature. With proper care, a set of data can be obtained that have constant values of n over a limited temperature range. Moreover, the Avrami plots are straight lines from very low degrees of conversion (0.2%) and show a small decrease at approximately constant conversion (70–80%), as shown in *Figures 4* and *7*. Using different experimental techniques our results indicate that the most careful data acquisition and analysis always lead to values of the Avrami exponent close to 2.

As shown in *Figure 7* many Avrami analyses show a lower slope at conversions over 70–80%. This has been ascribed to secondary crystallization within the spherulites. However, such breaks implicitly indicate that the wrong value for the 100% conversion of the primary crystallization that is being studied has been chosen. We have repeated the Avrami analysis with other values of the 100% conversion of the primary crystallization and generally have found that this has a small effect on n and k. Such correction would only be allowed if the secondary crystallization is consecutive to the primary one. This is not known. Indeed, if the secondary crystallization occurs concurrently with the primary one, a very difficult analytical problem would result. For these reasons, this correction was omitted.

The value of $n = 2$ obtained for the Avrami exponent is not consistent with spherulitic growth ($n = 3$). The exact reason for this low value is not known. It is conceivable that rather disc-like spherulites form as proposed by Lovinger and Davis[24], which could lead to apparent $n = 2$ Avrami kinetics. Kinetics of crystallization of commercial samples has led to variable values of n usually closer to 3[3,4,11,19]; others found 2.4 (ref. 20). Comparison of crystallization rates can nevertheless be made on the basis of crystallization half-times $t_{1/2}$.

Commercial samples with dilute solution viscosities (intrinsic or inherent) of about 1 dl g^{-1} have $M_n \approx 15\,000$ and $M_w \approx 30\,000$–$40\,000$[8,10,11]. These samples have crystallization half-times between our samples 2C/1 ($M_n = 14\,500$) and 2D/1 ($M_n = 7000$), for crystallization both from the glass[3,4] and from the melt[3,4,11,19]. This suggests that comparison of rates of crystallization of samples of wide molecular-weight distribution can be made on the basis of M_n[47]. Only the values of $t_{1/2}$ quoted by Jog[20] are three times lower than those for 2D/1. Unfortunately, no molecular characterization on his sample or details of the thermal treatment are provided.

According to the Hoffman–Lauritzen model of polymer crystallization:

$$K_g(\mathrm{II}) = \frac{2b\sigma\sigma_e T_m^\circ}{\rho \Delta h_f k} \qquad K_g(\mathrm{III}) = \frac{4b\sigma\sigma_e T_m^\circ}{\rho \Delta h_f k} \tag{6}$$

where the (II) indicates that we assume regime II crystallization in which secondary nucleation and spreading over the substrate compete with each other. With regime II, the numerical coefficient in equations (6) is 2. At lower temperatures regime III is observed. Secondary nucleation is very fast and spreading is limited to small niches. The coefficient is 4 in that case.

The experimental results of *Figure 9* indicate that, at low temperature, crystallization is according to regime III but above about 298°C according to regime II. The average values of $K_g(\mathrm{II})$ and $K_g(\mathrm{III})$ lead to the ratio $K_g(\mathrm{III})/K_g(\mathrm{II}) \approx 2$. The crystallization rate data for our PEEK fractions have been analysed in terms of regime II and III crystallization kinetics[42]. The study of the crystallization of PEEK is always performed at large undercooling. In this study $T_c/T_m^\circ = 0.89$ for the highest crystallization temperature. Moreover, the maximum crystallinity reached is only about 50%. Both observations exclude regime I conditions.

The analysis of the data according to equation (5) and the conclusions drawn from it in terms of regime behaviour may depend on underlying assumptions[39,42]. First, there is the choice of a set of $T_\infty = T_g - 55$ and $U^* \approx 4500$ cal mol^{-1}. They are taken from the crystallization results obtained from the glass. However, in the literature on crystallization kinetics, another set, $T_\infty = T_g - 30$ with $U^* \approx 1500 \pm 300$ cal mol^{-1}, is often preferred[42]. When our data on the crystallization from the glass are analysed with $T_\infty = T_g - 30$, the plots analogous to *Figure 5* are slightly curved. Without too much effort, best slopes yield values of U^* between 1800 and 2100 cal mol^{-1}. This alternative set of T_∞ and U^* has been used to reanalyse the data obtained on crystalliza-

Table 5 K_g(II) and/or K_g(III)

	$T_\infty = T_g - 55°C$ $U^* \approx 4500$ cal mol^{-1} $T_m^\circ = 395°C$	$T_\infty = T_g - 30°C$ $U^* \approx 1800$ cal mol^{-1} $T_m^\circ = 395°C$	$T_\infty = T_g - 55°C$ $U^* \approx 4500$ cal mol^{-1} $T_m^\circ = 406.8 - 1.7 \times 10^5/M_n$	
Sample	K_g (10^6 K^2)	K_g (10^6 K^2)	T_m° (°C)	K_g (10^6 K^2)
4D/1	3.22	2.79	404.0	3.71
1A22/1	3.00	2.57	401.9	3.30
1B/1′	2.30	2.21	398.8	2.07
	1.29	1.33		1.23
2C/1	1.28	1.31	395.1	1.21
1C/1	1.50	1.42	387.9	1.25
2D/1	1.32	1.33	382.2	1.24
$\frac{K_g(III)}{K_g(II)}$	2.11	1.87		2.46

tion from the melt. The new values of K_g(II) and/or K_g(III) are given in *Table 5* for comparison with those of the original analysis. The absolute values of K_g(III) are 15% lower, while the values of K_g(II) are little affected. The ratio $K_g(III)/K_g(II)$ is still close to 2. The transition from regime II to regime III in 1B/1′ occurs around 293°C. It is therefore concluded that the basic conclusions drawn from the kinetic data are little affected by the exact values of a consistent set of T_∞ and U^*. Note that when T_∞ is increased, U^* decreases. T_∞ and U^* are not independent; it is therefore not allowed to keep one constant and widely vary the other.

Results on the effect of T_∞ and U^* on the kinetics of crystallization from the melt and analysis in terms of regimes II and III are inconclusive. Lovinger *et al.*[39] found that the choice of a set of values of T_∞ and U^* did not affect the temperature of transition from regime II to regime III. However, they observed that the ratio $K_g(III)/K_g(II)$ changed from 2 to 3 when $T_\infty = T_g - 30$ was changed to the WLF values. Absolute values of K_g(III) were thereby affected but K_g(II) was relatively unaffected. Phillips *et al.*[43] preferred the WLF set of values for T_∞ and U^*, which yields regime II to regime III transitions and $K_g(III)/K_g(II)$ between 1.63 and 1.83. The empirical values, $T_\infty = T_g - 30$, $U^* = 1500$ cal mol^{-1}, sometimes erase the transition. Their results suggest that the transition temperature could be very molecular-weight-dependent, being lower for lower-molecular-weight samples. In poly(pivalolactone), the regime II to regime III transition was little affected by the different choices of T_∞ and U^*, in particular $K_g(III)/K_g(II)$ was close to 2 (ref. 48).

The analysis of the kinetic results may also depend on the values of T_m°. We have used the value found by Blundell ($T_m^\circ = 395°C$) based on the extrapolation of the lower melting temperature to infinite lamellar thickness[1]. This assumes that the lower melting temperature is associated with the originally formed lamellae. This point has been questioned[17]. Lee and Porter have tried to avoid reorganization of lamellae during d.s.c. scans by using faster heating rates[8]. They suggest that the lower melting temperature used by Blundell leads erroneously to $T_m^\circ = 420°C$. When, at fast heating rates, a single T_m is observed, they find $T_m^\circ = 384°C$[8]. The same authors had previously found $T_m^\circ = 389 \pm 4°C$ from a Hoffman–Weeks plot of the high-temperature melting peak when crystallization or annealing is performed above 300°C[10]. Cebe[5] found this method not appropriate for accurate determination of T_m°. The correct value of T_m° is therefore still somewhat uncertain.

To our knowledge nobody has investigated the possible MW dependence of T_m° of PEEK. Efforts in this direction are continuing. A dependence of T_m° on molecular weight of the related poly(phenylene sulphide) (PPS) has been observed[39,49]. The number of data points are few and the molecular-weight range is too small. However, it seems reasonable to assume that T_m° will depend on MW^{-1}, probably M_n^{-1}, since low-molecular-weight fractions will, by necessity, form less 'infinitely thick' lamellae. For PPS, the available data fit $T_m^\circ = (317 \pm 3) - 1.7 \times 10^5 M_n^{-1}$ (°C). When we use the same slope and assign $T_m^\circ = 395°C$ to a PEEK fraction with $M_n = 15\,000$ (2C/1), values of T_m° for the individual samples can be calculated. They are given in the last but one column of *Table 5*. Note that a large variation of T_m° is introduced by this procedure. The individual values of T_m° were used to recalculate the abscissa of *Figure 9*. Values of K_g(III) and K_g(II) are given in the last column of *Table 5*. It can be seen that the absolute values of K_g(III) increase and K_g(II) decrease. As a result $K_g(III)/K_g(II) = 2.5$. The transition temperature itself is little affected.

According to equations (6) values of K_g can be used to calculate the product $\sigma\sigma_e$. With $b = 4.68 \times 10^{-8}$ cm, the chain thickness in the crystal growth direction, $\Delta H_f = 130$ J g^{-1}, $\rho = 1.4$ g cm^{-3} (values from ref. 1) and k the Boltzmann constant, one finds from equations (6) and the values of K_g given above that $\sigma\sigma_e$, the product of the lateral and fold surface free energies, varies from 4.6×10^3 to 6.5×10^3 erg^2 cm^{-4}. Assuming a value of $\sigma = 38$ erg cm^{-2} (ref.1), we find from K_g(III) that $\sigma_e = 121$–170 erg cm^{-2} and increases slightly with molecular weight. From K_g(II) we obtain $\sigma_e = 140$ erg cm^{-2}.

The surface free energy terms, σ and σ_e, will be discussed in the following paper in which a microscopic study of the spherulitic growth of the same fractions of PEEK is described[50].

It is worth mentioning that a single straight line could have been drawn for sample 1B/1′ in *Figure 9*. This would eliminate the regime II–regime III transition and result

in a continuous increase in the product $\sigma\sigma_e$ as a function of molecular weight. This will be discussed also in the following paper.

It is worth speculating that the possible transition from regime III to regime II crystallization behaviour at about 300°C may be related to some observations made on annealed PEEK samples. Isothermal crystallizing or annealing PEEK below 300°C always produces a double melting endotherm in an ordinary d.s.c. run (scan at 10 or 20°C min^{-1}). The lower melting temperature is approximately 15°C above the annealing temperature, the higher melting one is constant around 330°C[3,10,14]. Obviously, if some recrystallization occurs during the d.s.c. run, it can only be a fast process and is limited to be a reorganization within regime III. Long-time annealing above 300°C results in two melting endotherms: the first one is still about 15°C above the annealing temperature but the second one increases also with the annealing temperature, albeit at a slower rate[5,10,14]. Annealing above 300°C may produce some crystals formed in regime II fashion. These crystals are expected to be more perfect and to melt at higher temperature.

REFERENCES

1 Blundell, D. J. and Osborn, B. N. *Polymer* 1983, **24**, 953
2 Blundell, D. J. *Polymer* 1987, **28**, 2248
3 Kemmish, D. J. and Hay, J. N. *Polymer* 1985, **26**, 905
4 Cebe, P. and Hong, S.-D. *Polymer* 1986, **27**, 1183
5 Cebe, P. *J. Mater. Sci.* 1988, **23**, 3721
6 Cebe, P. *Polym. Eng. Sci.* 1988, **28**, 1192
7 Cebe, P. *Polym. Compos.* 1988, **9**, 271
8 Lee, Y. and Porter, R. S. *Macromolecules* 1989, **22**, 1756
9 Lee, Y. and Porter, R. S. *Polym. Eng. Sci.* 1986, **26**, 633
10 Lee, Y. and Porter, R. S. *Macromolecules* 1987, **20**, 1336
11 Lee, Y. and Porter, R. S. *Macromolecules* 1988, **21**, 2770
12 Velinaris, C. N. and Seferis, J. C. *Polym. Eng. Sci.* 1986, **26**, 1574
13 Ostberg, G. M. K. and Seferis, J. C. *J. Appl. Polym. Sci.* 1987, **33**, 29
14 Cheng, S. Z. D., Cao, M. Y. and Wunderlich, B. *Macromolecules* 1986, **19**, 1868
15 Cheng, S. Z. D. and Wunderlich, B. *J. Polym. Sci., Polym. Phys. Edn* 1986, **27**, 1755
16 Cheng, S. Z. D., Linn, S., Judovits, L. H. and Wunderlich, B. *Polymer* 1987, **28**, 10
17 Bassett, D. C., Olley, R. H. and Al Raheil, I. A. M. *Polymer* 1988, **29**, 1745
18 Chang, S. S. *Polym. Commun.* 1988, **29**, 138
19 Day, M., Suprunchuk, T., Cooney, J. D. and Wiles, D. M. *J. Appl. Polym. Sci.* 1988, **36**, 1097
20 Jog, J. F. and Nadkarni, V. M. *J. Appl. Polym. Sci.* 1986, **32**, 3317
21 Chang, S.-S. *Polym. Commun.* 1988, **29**, 138
22 Kumar, S., Anderson, D. P. and Adams, W. *Polymer* 1986, **27**, 329
23 Deslandes, Y., Day, M., Sabir, N. F. and Suprunchuk, T. *Polym. Compos.* 1989, **10**, 360
24 Lovinger, A. J. and Davis, D. D. *J. Appl. Phys.* 1985, **58**, 2843
25 Lovinger, A. J. and Davis, D. D. *Polym. Commun.* 1985, **26**, 322
26 Lovinger, A. J. and Davis, D. D. *Macromolecules* 1986, **19**, 1861
27 Dawson, P. C. and Blundell, D. J. *Polymer* 1980, **21**, 577
28 Rueda, D. R., Ania, F., Richardson, A., Ward, I. M. and Balta-Calleja, F. J. *Polym. Commun.* 1983, **24**, 258
29 Wakelyn, N. T. *Polym. Commun.* 1984, **25**, 305
30 Wakelyn, N. T. *J. Polym. Sci. (C) Polym. Lett.* 1987, **25**, 25
31 Hay, J. N., Kemmish, D. J., Langford, J. I. and Rae, A. I. M. *Polym. Commun.* 1984, **25**, 175
32 Hay, J. N., Kemmish, D. J., Langford, J. I. and Rae, A. I. M. *Polym. Commun.* 1985, **26**, 283
33 Hay, J. N., Kemmish, D. J. and Lloyd, J. R. *Polymer* 1989, **30**, 489
34 Hay, J. N. and Kemmish, D. J. *Polym. Commun.* 1989, **30**, 77
35 Frantini, A. V., Cross, E. M., Whitaker, R. B. and Adams, W. W. *Polymer* 1986, **27**, 861
36 Yoda, O. *Polym. Commun.* 1985, **26**, 16
37 Mohanty, D. K., Lowery, R. C., Lyle, G. D. and McGrath, J. E. *SAMPE Symp.* 1987, **32**, 408
38 Roovers, J., Cooney, J. D. and Toporowski, P. M. *Macromolecules* 1990, **23**, 1611
39 Lovinger, A. J., Davis, D. D. and Padden, F. J. *Polymer* 1985, **26**, 1595
40 Ergoz, E., Fatou, J. G. and Mandelkern, L. *Macromolecules* 1972, **5**, 147
41 Ferry, J. D. 'Viscoelastic Properties of Polymers', 3rd Edn, Wiley, New York, 1980
42 Hoffman, J. D., Davis, G. T. and Lauritzen, J. I., Jr 'Treatise on Solid State Chemistry' (Ed. N. B. Hannay), Plenum Press, New York, 1976, Vol. 3, p. 568
43 Phillips, P. J. and Vatansever, N. *Macromolecules* 1987, **20**, 2138
44 de Gennes, P. G. 'Scaling Concepts in Polymer Physics', Cornell University Press, Ithaca, NY, 1979, p. 227
45 Roovers, J. unpublished results
46 Deslandes, Y. and Day, M. unpublished results
47 Hoffman, J. D. *Polymer* 1983, **24**, 3
48 Roitman, D. B., Marand, H., Miller, R. L. and Hoffman, J. D. *J. Phys. Chem.* 1989, **93**, 6919
49 Lopez, L. C. and Wilkes, G. L. *Polymer* 1988, **29**, 106
50 Deslandes, Y., Sabir, F.-N. and Roovers, J. *Polymer* 1991, **32**, 1267